JOURNAL OF SYNCHROTRON RADIATION

ISSN 1600-5775

Received 26 November 2019
Accepted 22 April 2020

Edited by S. Svensson, Uppsala University, Sweden

Keywords: fourth-generation storage ring; EUV; free-electron laser.

Demonstration of a ring-FEL as an EUV lithography tool

Jaeyu Lee,[a] G. Jang,[b] J. Kim,[c] B. Oh,[a] D.-E. Kim,[a] S. Lee,[a] J.-H. Kim,[a] J. Ko,[a] C. Min[a] and S. Shin[a]*

[a]Pohang Accelerator Laboratory, POSTECH, Pohang, Gyungbuk 37673, Republic of Korea, [b]Department of Physics, POSTECH, Pohang, Gyungbu 37673, Republic of Korea, and [c]SLAC National Accelerator Laboratory, Menlo Park, CA 94025, USA. *Correspondence e-mail: tlssh@postech.ac.kr

This paper presents the required structure and function of a ring-FEL as a radiation source for extreme ultraviolet radiation lithography (EUVL). A 100 m-long straight section that conducts an extremely low emittance beam from a fourth-generation storage ring can increase the average power at 13.5 nm wavelength to up to 1 kW without degrading the beam in the rest of the ring. Here, simulation results for a ring-FEL as a EUVL source are described.

1. Introduction

Extreme ultraviolet radiation lithography (EUVL) is a candidate to succeed 193 nm immersion lithography to pattern critical layers during the manufacture of integrated circuits. Therefore, radiation sources for EUVL are currently being developed. Advances in the power and reliability of laser-produced plasma (LPP) sources have enabled their application to next-generation technology development programs, but slow progress in LPP sources has delayed the adoption of EUV technology in high-volume manufacturing. In addition, increasing source requirements are driving the source community to consider pushing LPP technology beyond its current target of 250 W, or even higher.

A free-electron laser (FEL) (Kim, 1986) that uses a storage ring (ring-FEL) (Murphy & Pellegrini, 1985) is a candidate high-brightness radiation source for EUVL. A ring-FEL has the advantage of high average power, but electron bunches in the storage ring have a low peak current and a high energy spread. Therefore, many techniques have been developed to obtain FEL lasing by using the storage-ring electron beam. Methods to overcome the low peak current include the use of a transverse gradient undulator (TGU) (Smith *et al.*, 1979) and the application of bunch compression to increase the peak current (Feng & Zhao, 2017). However, those techniques must bypass the electron beam from the ring; this strategy reduces the FEL repetition rate, whereas EUVL requires a high average radiation power, so the high repetition rate of a storage ring is a great advantage. Recent work on steady-state self-amplified spontaneous emission FELs proved that a bypass is not necessary for the FEL in a storage ring at EUV and soft X-ray wavelengths (Huang *et al.*, 2008). Here we show that sufficient EUV FEL lasing for EUVL can be obtained using the electron bunch of a low-emittance ring without beam manipulation or a bypass beamline.

A fouth-generation storage ring (4GSR) that uses a multi-bend achromat (MBA) lattice concept may be able to surpass

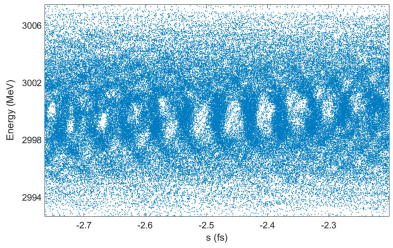

Table 1
Main parameters of the PAL-4GSR nominal lattice.

Parameter	Value	Unit
Energy	3	GeV
Emittance (flat / round)	80 / 58	pm
Circumference	570	m
Tune (x / y)	47.545 / 18.203	–
Natural chromaticity (x / y)	−96.0 / −57.9	–
Radiation loss per turn	0.468 (without insertion device)	MeV
Momentum compaction	1.45×10^{-4}	
Damping partition (H / V / L)	1.82 / 1.00 / 1.18	
Damping time (H / V / L)	13.37 / 24.35 / 20.66	ms

the brightness and coherence that are attained using present third-generation storage rings (3GSRs). 4GSRs have decreased beam emittance to a few hundred picometers, or even to $\leq$100 pm (Liu *et al.*, 2013; Steier *et al.*, 2016; see also MAX IV Conceptual Design Report, http://www.maxlab.lu.se/maxlab/max4/index.html; ESRF-EBS, http://indico.psi.ch/conferenceDisplay.py?confId=5589; APS Upgrade, https://www1.aps.anl.gov/aps-upgrade; Spring-8-II Conceptual Design Report, http://rsc.riken.jp/eng/index.html).

A ring-FEL that uses a 4GSR has extremely low electron-beam emittance, and can therefore generate high average power that is suitable for EUVL. However, uses for EUVL are impeded by relatively large energy spread and low peak current. By applying a 10 nC camshaft bunch, a low-emittance electron beam with 250 A peak current is successfully generated. As a result, the average power at 13.5 nm wavelength from a ring-FEL has been increased to 1 kW. In this paper, we describe the start-to-end simulation of a ring-FEL as a beam source for EUVL. Section 2 introduces the characteristics of the PAL-4GSR lattice. Section 3 describes the ring-FEL output characteristics. Section 4 presents conclusions.

2. PAL-4GSR lattice design for a ring-FEL

The PAL-4GSR (Kim *et al.*, 2019) storage ring (Table 1) is a hybrid seven-bend achromat (H7BA) lattice with a horizontal emittance of 90 pm. The ring is 570 m in circumference and is composed of 20 symmetrical cells. The straight section is 6.5 m long to accommodate two SCRF modules. The PAL-4GSR lattice contains a 2 T super-bend magnet in the central dipole to produce radiation that has a critical energy of 12 keV.

ESRF-II and APS-U lattices were adopted in the PAL-4GSR lattice. The dispersion was deliberately enlarged between the first and second dipoles, and between the sixth and seventh dipoles. All chromatic sextupoles were located in this dispersion bump region to reduce the strength required to control the chromaticity. The betatron phase advances between the two dispersion bumps were set to $\Delta\varphi_x \simeq 3\pi$ in the horizontal plane and $\Delta\varphi_y \simeq \pi$ in the vertical plane. As a result, non-chromatic effects of the sextupoles are cancelled out naturally. To minimize natural emittance, five-step longitudinal gradient dipoles and reverse bending magnets were used.

The storage-ring RF system includes two SC cavities, each driven by a klystron that delivers a continuous wave of up to 240 kW at 500 MHz. The accelerating voltage in the main RF cavity is 2.15 MV to realize a bucket height of ∼5%. The stored beam has RMS bunch length of 8 mm with the assumption of a third harmonic cavity for bunch prolongation, and natural energy spread of 0.1%. When the beam current is 400 mA in multi-bunch operation mode, the emittance increase due to intra-beam scattering is 10% in round-beam mode.

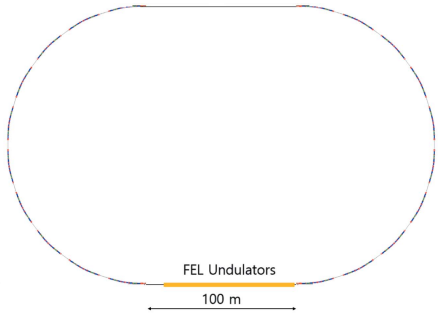

Figure 1
Ring-FEL configuration.

The ring-FEL option of PAL-4GSR requires two 100 m-long straight sections for FEL undulators (Fig. 1). Inserting the two long straight sections in the PAL-4GSR nominal lattice changes the PAL-4GSR shape from ring to racetrack; the circumference becomes 770 m and the revolution time increases to 2.57 µs. To obtain high peak current without any bunch compressing, we increase the bunch charge to 10 nC and turn off the third-harmonic cavity. Bunch length is slightly increasing along the bunch charge, so for the ring-FEL option we use bunches with a length of 4.2 nm and total charge of 10 nC. Peak current is ∼280 mA and energy spread is 0.1%. Due to intra-beam scattering (IBS) (Kubo *et al.*, 2005), a high-charge bunch has rather high emittance (Fig. 2). To reduce IBS, we use round-beam mode. The emittance of a zero-charge beam is set to 58 pm for the round-beam mode. The emittance of the 10 nC round beam is ∼133 pC and we set the beam emittance as 200 pC to allow margin for error. A charge of 10 nC translates to a bunch current of 4 mA. We set the filling pattern for the ring-FEL option as 80 camshaft bunches, so then the total current is 320 mA. Considering the heating

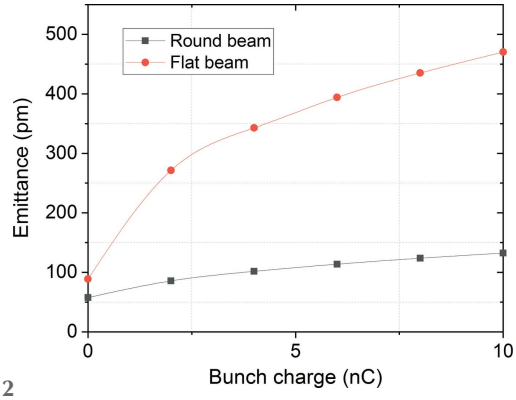

Figure 2
Emittance increase by the intra-beam scattering effect. For 10 nC round beam, the emittance increases from 58 pm to 130 pm

effect of the camshaft bunches, we choose a total current that is lower than the nominal operation mode. As a result, the FEL repetition rate is 31.2 MHz, which greatly exceeds that of an XFEL, which is ∼100 Hz for normal conducting RF and 1 MHz for superconducting RF, so a ring-FEL has a great advantage.

We should consider that using a 100 m-long undulator consumes large RF power. The total power from the undulator spontaneous radiation is calculated as

$$P_{\rm o} = 0.633 E^2 B_0^2 L I, \quad (1)$$

where E [GeV] is electron energy and B_0 [T] is undulator peak field, L [m] is the total undulator length and I [A] is the beam current. In our case, the FEL undulator has $P_{\rm o}$ = 382.8 kW. Considering that one superconducting RF module provides 240 kW, a ring-FEL option requires two additional superconducting RF modules.

3. Ring-FEL output characteristics

The required FEL power to achieve 1 kW average EUV power can be calculated from the measured bunch length and repetition rate. A bunch length of 4.2 mm and repetition rate of 31.2 MHz yield a bunch averaged FEL power of 0.916 MW. In a conventional linac X-ray FEL, bunch-averaged FEL power is on the order of gigawatts, so the required FEL power for the EUVL in a ring-FEL is relatively low because of the high repetition rate of the storage ring. Despite the large energy spread and low peak current of the electron beam in the storage ring, a megawatt-level FEL is easily achievable in the EUV regime if a 100 m undulator is used (Fig. 3).

Due to the high repetition rate of the ring-FEL option of PAL-4GSR, its parameters (Table 2) enable an average FEL power that is sufficiently high at the saturation point. To reduce degradation of electron beam quality and the undulator length, we will stop the FEL lasing before the saturation point. Currently, the demanding laser wavelength for the EUVL is 13.5 nm. However, in the near future a reduction in wavelength will be needed; therefore, we consider use of a variable gap undulator to change the FEL wavelength from

Table 2
Parameters of the ring-FEL option of PAL-4GSR.

Parameter	Value	Unit
Energy	3	GeV
RMS bunch length	14	ps
Bunch charge	10	nC
Peak current	280	A
Relative energy spread	0.001	–
Repetition rate	31.2	MHz
Undulator period	4.4	cm
Magnet full gap	6.81 / 10.27	mm
FEL wavelength	13.5 / 7	nm
Saturation peak power	95 / 53	MW
Saturation length	109.8 / 156.3	m
Average FEL power (at saturation)	103 / 58	kW

13.5 nm to 7 nm. This decrease in wavelength will decrease FEL power and increase the saturation length, but the average power will remain >1 kW. Assuming that the electron beam parameters of the storage ring are invariant including the FEL undulator, an average power of 100 kW is achieved before 100 m. However, the electron beam parameter is affected by the FEL radiation and we should identify the equilibrium condition of the ring-FEL configuration.

The FEL simulation was conducted using the code *Genesis 1.3* (Reiche, 1999). Time-dependent simulation shows the evolution of the microbunching. The electron beam began to form microbunches at >135 m from the undulator (Fig. 4). Microbunching is the key to FEL lasing, but can damage a storage ring.

Energy loss and increase in energy spread also degrade the electron beam of the FEL lasing. The energy loss of the 3 GeV electron beam is 1.5 keV per turn, which is negligible compared with the energy loss of the FEL (∼1 MeV per turn) (Fig. 5). Of this 3 GeV electron beam, 343 keV per turn is caused by bending-magnet radiation except the insertion devices. The relative energy spread is increased 0.0001% per one turn by FEL generation (Fig. 6). Therefore, we will reduce the harmful effect on the storage ring by extracting the electron beam in the undulator before saturation. The bunch-averaged FEL power along the undulator begins to increase exponentially at ∼40 m; the energy spread also begins to

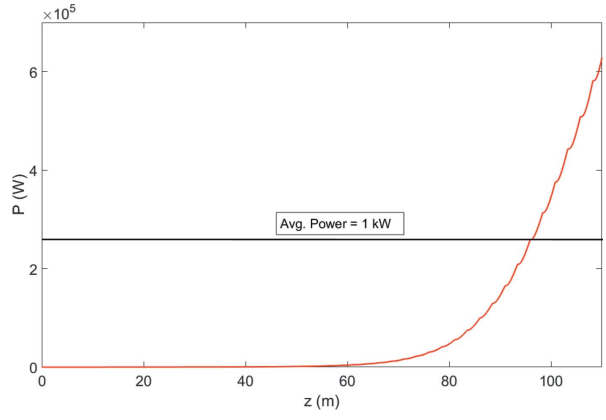

Figure 3
FEL power along undulator; average power of 1 kW is achieved before 100 m.

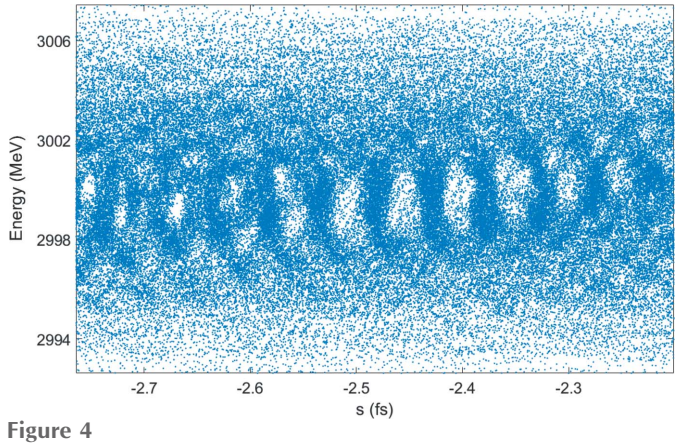

Figure 4
Microbunching after 135 m undulator.

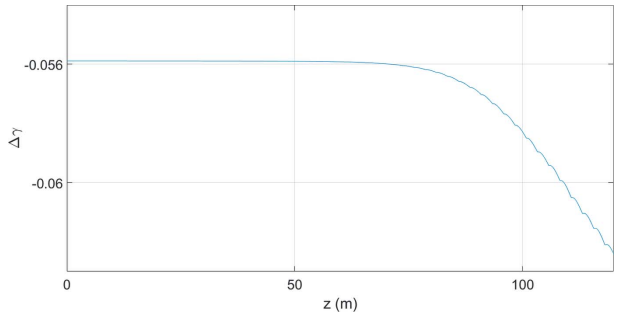

Figure 5
FEL energy loss along the undulator. Energy loss per turn is 1.5 keV, which is negligible because the energy loss of the storage ring is ∼1 MeV per turn.

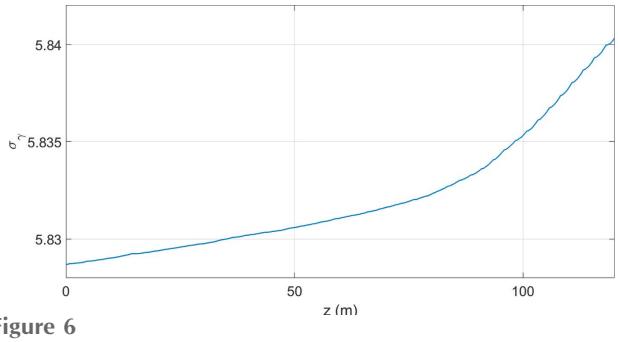

Figure 6
FEL energy spread along the undulator. Energy spread increase per turn is ∼0.0001%; this small increase affects the equilibrium energy spread of the storage ring and degrades FEL power.

increase, but remains low (Fig. 7). Undulator length is determined by the required EUV radiation power, not by the saturation length.

To examine the effect of the FEL undulator on the storage ring, a full particle tracking is needed for several thousand turns. In addition, at least 1000 particles per 13.5 nm must be tracked to deliver the microbunching property. The RMS bunch length is 4 mm and the FEL wavelength is 13.5 nm, so more than one million microbunches occur. If we track 1000 particles per microbunch, then one billion particles must be tracked. Therefore, a full particle tracking for several thousand turns requires too much computing power. We rather examine the microbunching effect of one microbunch in the peak current position and examine the energy and the energy spread effect of the FEL to the rest of the ring. We also examine the emittance change by the FEL through the damping wiggler theory.

We used the code *Elegant* (Borland, 2000) to conduct a particle-tracking simulation of the ring, excluding the FEL part. The microbunching is washed out before the first turn (Huang *et al.*, 2008), so we focused on the energy and energy spread effect. The energy-loss effect that was described in the previous section is negligible compared with that in a normal wiggler. The energy spread is the key to the interaction between the ring and the FEL; this effect has been well investigated previously (Huang *et al.*, 2008). The maximum radiation power is determined by the electron beam power, the Pierce parameter, the longitudinal damping time, and the energy spread without the FEL. In our case, the maximum radiation power is ∼1 kW which is our target FEL power. Storage-ring theory suggests that equilibrium energy spread is determined when the quantum excitation effect and the longitudinal damping effect have the same strength but opposite directions. The equilibrium energy spread σ_e considering the FEL effect is estimated as (Huang *et al.*, 2008)

$$\sigma_e = \left[\sigma_0^2 + \frac{\Delta(\sigma^2)_{\rm FEL}\,\tau_s}{2T_0}\right]^{1/2}, \qquad (2)$$

where σ_0 is the relative energy spread in the absence of the FEL and $\Delta(\sigma^2)_{\rm FEL}$ is an increase of the square of the relative energy spread by single FEL lasing, τ_s [ms] is the longitudinal damping time and T_0 [μs] is the revolution time. In our case, $\sigma_0 = 10^{-3}$, $\Delta(\sigma^2)_{\rm FEL} = 2 \times 10^{-9}$, $\tau_s = 10$ ms, $T_0 = 2.57$ μs. The calculated equilibrium relative energy spread was $\sigma_e = 2.2 \times 10^{-3}$, which noticeably degrades the beam property, and thereby reduces the FEL power and increases the saturation length. Because of this energy spread increase, we introduce the seeded FEL scheme to compensate for the increase in energy spread.

To achieve 1 kW power, we conducted two FEL simulations. Both started with 10 kW pulsed seeding power, but the energy spread was 0.1% in the first simulation and 0.2% in the second. With 0.1% energy spread (Fig. 7), the average FEL power was 1 kW at about z = 63 m and energy spread increased at z = 63 m to ∼0.0001%, which is the same as in the no-seeding case. In contrast, with 0.2% energy spread (Fig. 8), which is expected for the equilibrium energy spread, 1 kW power was achieved at z = 80 m but the energy spread increased by only 0.00003%, and the energy spread started to decrease after z = 60 and became close to the initial value at z = 100 m. After z = 60 m, the energy spread decreased but the FEL power increased linearly. This result indicates that we could obtain 1 kW EUV FEL power while the equilibrium energy spread is below 0.2%

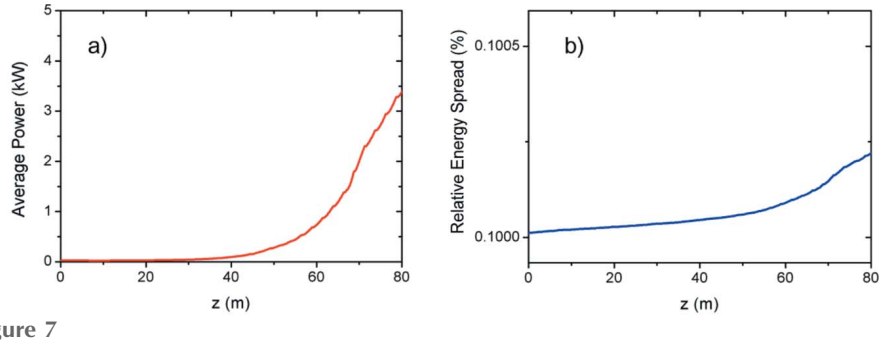

Figure 7
(*a*) FEL average power and (*b*) relative energy spread along the undulator with 10 kW pulsed seeding radiation and 0.1% initial energy spread. 1 kW average power is achieved before 80 m undulator length and energy spread increases by 0.0001%.

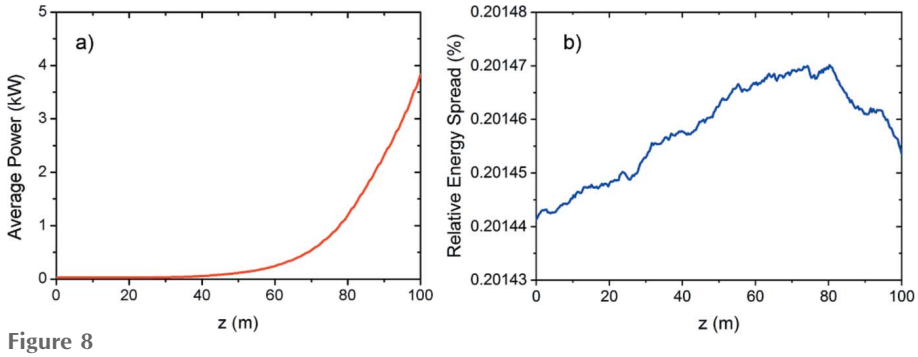

Figure 8
(*a*) FEL average power and (*b*) relative energy spread along the undulator with 10 kW pulsed seeding radiation and 0.2% initial energy spread. 1 kW average power is achieved before 100 m undulator length and energy spread increase is negligible.

with 10 kW pulsed seeding power and a 100 m-long undulator.

Many 3GSRs implement a damping wiggler to decrease the emittance (Jang *et al.*, 2020). A wiggler with a strong field in a non-dispersive section helps to reduce the equilibrium emittance. One can expect that the FEL undulator effects the storage ring similar to the damping wiggler. In our case, the undulator period is 4.4 cm and the peak magnetic field is 1.54 T; therefore the emittance reduction rate is ∼0.3 and the equilibrium emittance will change from 200 pm to 60 pm (Fig. 9).

In this simulation, we achieved 1 kW EUV power by using the seeded FEL scheme. A seeded FEL requires a source to seed the radiation. The required seeding radiation is 1 kW pulsed radiation that is synchronized with the electron beam. The average power of the seeding radiation is ∼40 W. The seeding methods of the seeded FEL are external seeding or self-seeding. For external seeding, a laser is generally used. If the external seeding source is difficult to obtain, the self-seeding scheme can be used (Feldhaus *et al.*, 1997). When a self-seeding scheme is used, the requirements for repetition rate and pulse length are easily achievable. Requirements for the external seeding laser are: 31 MHz repetition rate, 10 kW peak power, and 4 mm RMS pulse length. Currently, these requirements are not achievable. Therefore, two self-seeding schemes are considered to generate seeding radiation satisfying the requirement.

The traditional self-seeding scheme can be applied by adding another long undulator in the opposite long straight section of the race-track structure; one long undulator is for seeding radiation and the other is for the seeded FEL. The seeding FEL undulator is 60 m long and generates 10 kW FEL without degrading the energy spread.

Another scheme is to use a part of the FEL radiation as a seeding source. This approach is similar to the regenerative amplifier scheme (Nguyen *et al.*, 1999), but our scheme reflects only a small fraction of the FEL radiation. FEL peak power is >2.5 MW and the required seeding peak power is ∼10 kW, so the mirror reflects only 0.4% of the FEL radiation power and transmits the rest. To achieve timing, the number of camshaft bunches should be an integer divisor of the harmonic number of the storage rings. To further increase the FEL power, the undulator tapering method can be considered.

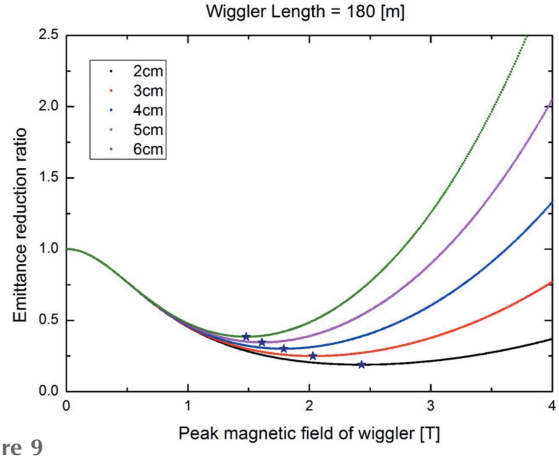

Figure 9
Emittance reduction ratio along with the peak magnetic field of the 180 m damping wiggler. The period of the damping wiggler is scanned from 2 cm to 6 cm. Ring-FEL configuration uses an 80 m-long undulator which has a 4.4 cm period and a 1.54 T peak field. It is close to an optimal condition as a damping wiggler.

4. Conclusion

The ring-FEL option of the PAL-4GSR is investigated for use in EUV lithography. The PAL-4GSR is a 3 GeV, 570 m, 58 pm low-emittance ring that is in its design stage. The ring-FEL option requires a change from ring structure to race-track structure with two 100 m-long straight sections. It also requires a dedicated operation mode that has 80 camshaft bunches with 10 nC single-bunch charge. The beam emittance of the camshaft bunch is increased by intra-beam scattering, but the damping wiggler effect of the FEL undulator reduces the beam emittance. The equilibrium beam emittance is <200 pm, so the ring-FEL dedicated mode is usable from the other storage-ring beamlines. Considering the energy spread increase from the FEL, we conclude that the seeding power is critical. With 10 kW seeding power, we achieved an average 1 kW EUV radiation as a EUV lithography source.

Funding information

This research was supported by the the Basic Science Research Program through the National Research Foundation of Korea (NRF-2019R1C1C1003412) and the Basic Science Research Program through the National Research Foundation of Korea (NRF-2019R1A2C1004862).

References

Borland, M. (2000). *Elegant: A Flexible SDDS-Compliant Code for Accelerator Simulation.* Technical Report LS-287. Advanced Photon Source, Argonne, IL, USA.

Feldhaus, J., Saldin, E. L., Schneider, J. R., Schneidmiller, E. A. & Yurkov, M. V. (1997). *Opt. Commun.* **140**, 341–352.

Feng, C. & Zhao, Z. (2017). *Sci. Rep.* **7**, 4724.
Huang, Z., Bane, K., Cai, Y., Chao, A., Hettel, R. & Pellegrini, C. (2008). *Nucl. Instrum. Methods Phys. Res. A*, **593**, 120–124.
Jang, G. *et al.* (2020). *J. Synchrotron Rad.* Submitted.
Kim, J., Jang, G., Yoon, M., Oh, B., Lee, J., Ko, J., Parc, Y., Ha, T., Kim, D., Kim, S. & Shin, S. (2019). *Phys. Rev. Accel. Beams*, **22**, 011601.
Kim, K. J. (1986). *Phys. Rev. Lett.* **57**, 1871–1874.
Kubo, K., Mtingwa, S. K. & Wolski, A. (2005). *Phys. Rev. ST Accel. Beams*, **8**, 081001.
Liu, L., Milas, N., Mukai, A. H. C., Resende, X. R., Rodrigues, A. R. D. & de Sá, F. H. (2013). *Proceedings of the Fourth International Particle Accelerator Conference (IPAC2013)*, 12–17 May 2013, Shanghai, China, pp. 1874–1876. TUPWO001.
Murphy, J. B. & Pellegrini, C. (1985). *Nucl. Instrum. Methods Phys. Res. A*, **237**, 159–167.
Nguyen, D. C., Sheffield, R. L., Fortgang, C. M., Goldstein, J. C., Kinross-Wright, J. M. & Ebrahim, N. A. (1999). *Nucl. Instrum. Methods Phys. Res. A*, **429**, 125–130.
Reiche, S. (1999). *Nucl. Instrum. Methods Phys. Res. A*, **429**, 243–248.
Smith, T. I., Madey, J. M. J., Elias, L. R. & Deacon, D. A. G. (1979). *J. Appl. Phys.* **50**, 4580–4583.
Steier, C., Byrd, J. M., De Santis, S., Nishimura, H., Robin, D., Sannibale, F., Sun, C., Venturini, M. & Wan, W. (2016). *Proceedings of the 7th International Particle Accelerator Conference (IPAC2016)*, 8–13 May 2016, Busan, Korea, pp. 2956–2958. WEPOW049.